

## Three-Cavity Circuit Studies of the Maryland Gyroklystron\*

C.D. Striffler, S. Tantawi, W. Main, B. Hogan, P.E. Latham, W. Lawson, U.-V. Koc,  
H.W. Matthews, G.S. Nusinovich, and V.L. Granatstein  
Laboratory for Plasma Research  
University of Maryland, College Park, MD 20742 USA

### Abstract

At the University of Maryland we have examined an X-Band TE<sub>01</sub> mode three-cavity gyrokystron circuit that includes a tunable buncher cavity. The system parameters are: 425 kV, 100-200 A, pulse length  $\sim 1 \mu\text{s}$ , operating frequency 9.85 GHz, and a beam alpha,  $v_{\perp}/v_z$ , in the range 0.7 - 1.0. This circuit produced a maximum power of 27 MW at 32% efficiency and a gain of 36 dB. We will summarize the major results of the three-cavity systems, including recent output cavity configurations that were to affect the post-cavity interaction.

### Introduction

We are developing a three-cavity gyrokystron to show the feasibility of this device as an RF driver for future advanced linear accelerators.<sup>1</sup> For these accelerators to achieve energies in the TeV range, over a thousand phase locked drivers will be required. For this reason, achieving high gain will be important and may require gyrokystrons with three or more cavities. Our early work focused on two-cavity gyrokystrons which gave promising results.<sup>2-6</sup> In this paper we will present the results of our three-cavity studies.<sup>7,8</sup>

A schematic diagram showing the major components of the system appears in Fig. 1 and the microwave circuit appears in Fig. 2. The magnetron injection gun (MIG) is designed to give optimum beam quality at 500 kV for 160 A and a velocity ratio  $\alpha \equiv v_{\perp}/v_{\parallel} = 1.5$ . Our modulator produces pulses with 1  $\mu\text{s}$  flat-top and we typically operate at 1 Hz rep-rate. Eight d.c. water-cooled pancake coils produces the axial magnetic

guide-field. These coils are powered by four separate power supplies so that we can adjust the magnetic compression of the beam and vary the magnetic field taper across the circuit. This system can operate up to 6.5 kG at the circuit.

The important features of the circuit, Fig. 2, are the remotely tunable buncher cavity and the lossy dielectrics. To tune the cavity we insert two metal rods (OD = 5.1 mm) from opposite sides of the cavity. The tip of the rods travels from the outer wall of the cavity to within 5 mm of the drift tube radius. Most of the 120 MHz of tunability occurs when the probes are extended well into the cavity. The lossy dielectrics are placed on the outer wall of the cavities to suppress unwanted modes and in the drift regions to damp unwanted oscillations and to provide isolation for the cavities.

Input power for the gyrokystron is supplied by a 100 kW pulsed magnetron capable of producing 2  $\mu\text{s}$  pulses. Forward and reverse power are monitored. Coupling varied from 20% to 50% depending on beam parameters.

### Experimental Results

The three-cavity tubes had three distinct departures from the two-cavity designs.<sup>3-6</sup> The first departure, of course, was the introduction of the tunable buncher cavity whose Q ( $\sim 270$ ) was defined solely by an alumino-silicate ring on the outer wall. The second change was to use exclusively alumino-silicate in the drift tubes and downtaper. The TE<sub>11</sub> attenuation was always superior to their non-porous counterparts, the TE<sub>01</sub> attenuation was adequate for cavity isolation at 9.85 GHz, and no outgassing problems were observed. The third difference was to use a lossy dielectric on the radial wall of the input

\*This work is supported by the U.S. Department of Energy.

cavity to achieve a  $Q$  of 250 and to modify the coupling slit.

All of the three cavity tubes had at least two distinct operating regimes controlled by the magnetic field taper. Figure 3 shows the axial variation of the magnetic guide field for these two regimes. The tapers which optimize each of the operating regimes vary slightly from tube to tube, so we give the range of tapers used. The steep taper has a 30-32% decrease and a field of 0.458 T in the output cavity, and the weak taper has a decrease of 17-22% and a field of 0.453-0.490 T in the output cavity. The two regimes were also affected differently by increased load reflections.

The primary difference in the four tubes examined is the geometry of the output cavities. Figure 4 shows the output cavity cross-section of each of the tubes. Tube 1, with a diffractive output cavity  $Q$  of 200, operated well at high input power, producing 23 MW at 27% efficiency and 31 dB gain. At low input power, instabilities limited operation to lower  $\alpha$  or lower beam power. This prevented operation at high gain and high power. We also observed that the tube produced higher power when operated with the calorimeter (2% reflection) as opposed to the anechoic chamber ( $< 0.1\%$  reflection).

We suspected that the downtaper instabilities observed in Tube 1 were suppressed with higher input power and thus we significantly increased the attenuation in the downtaper in Tube 2. We also suspected that the enhanced operation with a more reflective load indicated that a higher  $Q$  in the output cavity was necessary. At our optimum beam power (425 kV and 205 A) Tube 1 was operating at 5% of start oscillation current in the output cavity so we also increased the output cavity  $Q$  from 200 to 350 in Tube 2. With these changes Tube 2 achieved 50 dB saturated gain at 20 MW, and 36 dB at the high power point of 27 MW where the efficiency was 32%. The tube was able to operate stably with input power as low as 200 watts.

Ongoing numerical modeling of this device which considers only cavity modes has shown efficiencies from 21% to 38% depending on how the beam loading affects the cavity  $Q$ s and the

value of the pitch angle. The theoretical results<sup>9</sup> are not consistent with the beam  $\alpha$  predicted by the gun code.<sup>10</sup> Concerned that some of the interaction was occurring after the output cavity we decided to increase the length of the output cavity. The cavity could be lengthened while keeping the same operating frequency, either by reducing the radius, Tube 3, or by going to the second axial harmonic,  $TE_{012}$ , Tube 4. We also included a probe in the radial wall of the output cavity in Tubes 3 and 4 to directly monitor the cavity interaction.

For Tube 3, with an output cavity  $Q$  of 465, the best power and gain occurred at the same operating point and were 22 MW and 44 dB, respectively. In the weak taper regime the uncalibrated probe signal was directly proportional to the measurement made in the anechoic chamber. This suggests that the weak taper corresponds to an interaction in the output cavity. The probe indicated that for a strong taper the interaction occurs outside the output cavity.

The output cavity in Tube 4,  $Q \sim 700$ , had the same radius as both Tubes 1 and 2 and an output cavity lip thickness the same as Tube 2. The cavity length, which was almost twice that of Tubes 1 and 2, was intended for operation in the  $TE_{012}$  mode. The long length of the cavity caused the  $TE_{011}$  and similar lower order modes with one axial variation to have high  $Q$ , and hence low start oscillation currents ( $< 10$  A). To suppress these modes, a thin ring of lossy dielectric was placed on the axial mid-plane of the cavity. Cold tests showed that this ring did not affect the  $Q$  of the  $TE_{012}$  mode while substantially reducing the  $Q$  of all single axial variation modes. As in Tube 3, Tube 4 also displayed two regimes of operation as regards magnetic field taper. Tube 4 has a maximum output power of 22 MW.

In summary, at 425 kV, as expected from their similar designs, Tubes 1 and 2 have similar operation characteristics. The increased  $Q$  in Tube 2 allows it to operate slightly better in the current regime of 100-200 A. Tube 3 has similar performance properties at high currents,  $\sim 200$  A, but has substantially reduced performance for currents 100-180 A. Below 100 A, where large alphas could be achieved, the tube free-oscillated

at the operating frequency. Tube 4, which had the longest output cavity, had significantly lower efficiency than Tubes 1 and 2 throughout the entire current regime of 100-200 A. This tube operated better at lower voltages. The three cavity circuit has achieved similar results in power and efficiency as the two cavity circuit and has produced substantially higher gain. Questions still remain as to the lack of agreement between our theoretical modeling and the experimental results.

**Acknowledgment**

We wish to acknowledge the efforts of C. Bellamy, J. Cheng, O. Dajani, S. Demske, K. Lee, Q. Qian, M. Rimlinger, and V. Specht.

**References**

1. Proc. Int. Workshop on the Next Generation Collider, SLAC Report-335, Dec. 1988.
2. K. R. Chu, et al., IEEE Trans. Plasma Sci. Vol. PS-13, p. 424 (1985).
3. J. P. Calame, et al., J. Appl. Phys. Vol. 70, p. 2423 (1991).
4. W. Lawson, et al., Phys. Rev. Lett. Vol. 67, p. 520 (1991).
5. W. Lawson, et al., IEEE Trans. Plasma Science Vol. 20, No. 3, p. 216 (1992).
6. W. Lawson, et al., Proc. of this Conf.
7. S. Tantawi, et al., IEEE Trans. Plasma Science, Vol. 20, No. 3, p. 205 (1992).
8. W. Main, et al., Proc. Beams '92 Conf., Washington, DC, May 1992.
9. P. E. Latham, et al., Proc. Beams '92 Conf., Washington, DC, May 1992.
10. W. B. Herrmannsfeldt, SLAC Report-226, Nov. 1979.

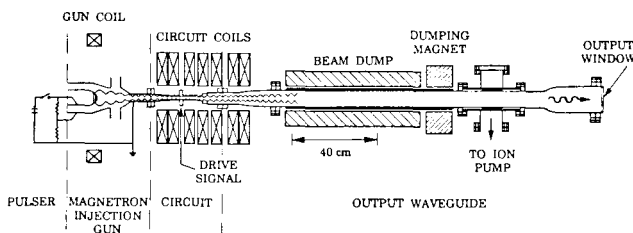


Figure 1. Schematic diagram of gyrokystron.

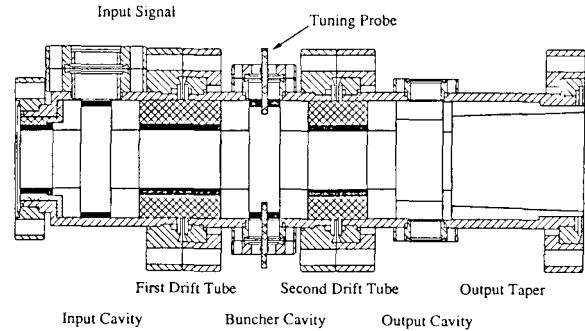


Figure 2. Diagram of microwave circuit.

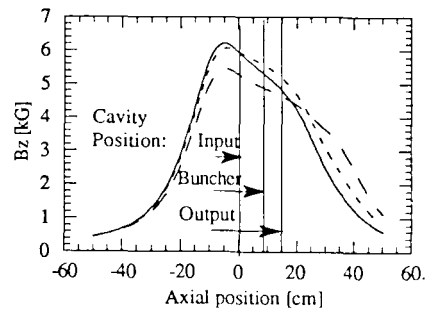


Figure 3. Axial variation of the guide field for the steep and weak tapers used in Tubes 2 and 3. Solid line — steep taper (30%), broken line - - - weak taper (17%) Tube 2, dotted line - - - - weak taper (22%) Tube 3.

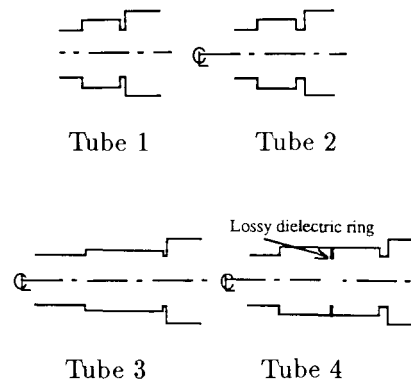


Figure 4. Cross-sectional diagrams of the output cavities of Tubes 1-4.